Caspase-independent commitment phase to apoptosis in activated blood T lymphocytes: reversibility at low apoptotic insult

Céline Dumont, Antoine Dürrbach, Nicolas Bidère, Matthieu Rouleau, Guido Kroemer, Ghislaine Bernard, François Hirsch, Bernard Charpentier, Santos A. Susin, and Anna Senik

Little is known about the mechanisms of programmed death triggered in T lymphocytes by stimuli that can bypass caspase activation. Anti-CD2 monoclonal antibody and staurosporine are such apoptosis inducers because they operate in the presence of broad-spectrum caspase inhibitors BOC-D.fmk and Z-VAD.fmk. A system was devised, based on the isolation according to density of activated blood T cells progressively engaged in the apoptotic process. This allowed definition of a sequence of caspase-dependent and caspase-independent apoptogenic events that are triggered by anti-CD2 and staurosporine. Thus, a commitment phase to apoptosis was defined that is entirely caspase independent and that is characterized by cell volume loss, partial chromatin condensation, and release into the cytosol and the nucleus of mitochondrial "apoptosis-inducing factor" (AIF). Committed cells were viable, displayed a high mitochondrial inner transmembrane potential ($\Delta\Psi$m), and lacked large-scale and oligonucleosomal DNA fragmentation. Mitochondrial release of AIF was selective because cyto-chrome c was retained in mitochondria of the very same cells. Mitochondrial release of cytochrome c occurred later, at the onset of the execution phase of apoptosis, concurrently with $\Delta\Psi$m collapse, poly (ADP-ribose) polymerase cleavage, and DNA fragmentation. The apoptogenic events of this commitment phase are reversible if the strength of the stimulus is low and of short duration. (Blood. 2000;96:1030-1038)

© 2000 by The American Society of Hematology

Introduction

Apoptosis or programmed cell death is a self-destruction process characterized by stereotyped ultrastructural changes including condensation of the nucleus and cytoplasm, membrane blebbing,[1] and external display of phosphatidylserine, a signal for recognition and engulfment of apoptotic cells by adjacent cells. In mammalian cells, the onset of apoptosis correlates with the activation of a family of cysteine proteases called caspases, which are constitutively expressed as inactive zymogens in the cytosol. Caspases constitute a potent machinery that cleaves crucial proteins of the nucleus and the cytoskeleton after Asp residues, and thus induce the phenotypic changes of apoptosis, including advanced chromatin condensation and internucleosomal DNA fragmentation (reviewed in Cryns and Yuan[2]). Evidence from an increasing number of experimental systems, using broad-spectrum caspase inhibitors, however, supports the notion that programmed cell death can also proceed in a caspase-independent manner, with stereotyped features [3-8] (reviewed in Borner and Monney[9]). For example, we have previously shown that in activated T cells exposed to some apoptotic inducers (anti-CD2 monoclonal antibody [mAb] or staurosporine) in the presence of Z-VAD.fmk or BOC-D.fmk, cell death occurs with only partial condensation of the chromatin and without internucleosomal DNA fragmentation, but maintains many other features of apoptosis, such as shrinkage of the cytoplasm and the nucleus, $\Delta\Psi$m collapse, membrane blebbing, and externalization of phosphatidylserine.[6] Remarkably, the expression of the adenovirus protein E4orfA in rodent fibroblasts induces apoptosis without even activating caspase-3.[7] The same is true for T lymphocytes subjected to cross-linking of the human immunodeficiency virus-1 (HIV-1) coreceptor CXCR4 by specific antibodies.[10] Chicken erythrocytes exposed to staurosporine die from apoptosis yet lack active proteases that cleave Z-VAD.afc, a classical caspase substrate, suggesting that caspase activation may not be involved at all in this system of cell death.[11]

The cellular mechanisms that account for caspase-independent programmed cell death are still elusive. In most cells subjected to an apoptotic insult in the presence of Z-VAD.fmk or BOC-D.fmk, dissipation of the mitochondrial inner transmembrane potential ($\Delta\Psi$m) is detected.[3,6,7] The loss of $\Delta\Psi$m is mediated by opening of the mitochondrial permeability transition (PT) pores[12] and is believed to be an early and irreversible event in the apoptotic process.[13] Caspase-unrelated death triggers or effectors might be released from mitochondria concomitantly with this mitochondrial dysfunction, thus triggering a caspase-independent cell death pathway. One critical effector might be apoptosis-inducing factor (AIF), a flavoprotein with striking homology with the reduced form of nicotinamide adenine dinucleotide oxidoreductases.[14] AIF resides in the intermembrane space of mitochondria and is translocated to the nucleus on opening of PT pores. When microinjected into cells in the presence of Z-VAD.fmk, recombinant AIF induces the same cellular changes as those observed during caspase-independent cell death.[14]

In most cells undergoing apoptosis, AIF may exert its apoptogenic effects in concert with mitochondrial factors involved in caspase activation, in particular with cytochrome c, a factor that is translocated from the intermembrane space of mitochondria to the cytosol after a death signal, and which, together with Apaf-1, dATP and caspase-9, activates pro-caspase-3 (reviewed in Cryns and Yuan[2] and Wolf and Green[15]). A number of other intermembrane space proteins are also released from mitochondria during apoptosis, including pro-caspase-9,[16] pro-caspase-3,[17] and the Hsp10 and Hsp60 chaperons, which assist pro-caspase-3 activation by upstream proteases.[18,19] Hence, an important issue is to know the sequence of caspase-dependent and caspase-independent cellular events that lead to the demise of cells during apoptosis. In activated T cells exposed to anti-CD2 or staurosporine, both caspase-dependent and a caspase-independent pathways of cell death are triggered.[6] In the present study, we sought to characterize the ordering of cellular events that define the commitment phase of apoptosis in these models. Progressive cell shrinkage and concomitant increase in cell density occur early after apoptotic induction.[20] This allows us to separate cells with increasing density, which represent successive stages of the apoptotic process, on discontinuous Percoll gradients.[21] Using this approach, we exposed large activated T cells to apoptosis-inducing stimuli, and thereafter fractionated them according to density. In each fraction, we monitored signs of apoptosis associated with mitochondrial alterations such as $\Delta\Psi$m collapse, release of cytochrome c and AIF, as well as signs of nuclear apoptosis such as chromatin condensation and DNA fragmentation. We also analyzed whether these events depended on caspase activation. For comparison, the same parameters were investigated in cells exposed to anti-CD95, a stimulus that directly triggers a caspase cascade in peripheral T lymphocytes.[22]

Materials and methods

Reagents

The CD2 mAb were GT2, T11$_1$, and D66.[6] Anti-CD95 mAb (CH-11) was from Immugenex Corp (Los Angeles, CA). Anti-PARP mAb (C2-10) was purchased from Dr G. G. Poirier (Montreal University, Montreal, Quebec, Canada). The mAbs recognizing the native form of cytochrome c (6H2.B4) or its denatured form (7H8.2C12) were from PharMingen (Becton Dickinson, Le Pont de Claix, France). Anticytochrome oxidase subunit II mAb (12C4-F12) was from Molecular Probes, (Interchim, Montluçon, France). Antiactin rabbit serum was from Sigma (Saint Quentin Fallavier, France). Rabbit anti-AIF was raised against a mixture of AIF peptides.[14] Z-VAD.fmk (benzyloxycarbonyl-Val-Ala-Asp[Ome]-fluoromethyl ketone) and BOC-D.fmk (Boc-Asp[Ome]-fluoromethyl ketone) were purchased from Enzyme Systems Products (Dublin, CA).

T lymphocyte isolation, culture conditions, and induction of cell death

Peripheral blood leukocytes were isolated from blood bank leukophoresis packs obtained from healthy volunteers (Blood Transfusion Center of Hôpital Saint Louis, Paris). After Ficoll-Isopaque density (d = 1.078) gradient centrifugation, adherent cells were removed by incubation on plastic dishes and passage over nylon wool columns. T lymphocytes (6×10^6 in the wells of 6-well flat-bottomed plates; Nunc, Roskide, Denmark) were stimulated for 4 to 5 days with the mitogenic GT2+T11$_1$ CD2 mAb pair (2 µg/mL) plus 100 U/mL interleukin-2 (IL-2) (Roussel Uclaf, Romainville, France). The death signals were given by T11$_1$+ D66 (2µg/mL), CH-11 (250 ng/mL), or staurosporine (0.1-0.5 µmol/L; from Sigma).

Percoll gradients

The T cells were fractionated on discontinuous Percoll gradients (Pharmacia Biotech, Saclay, France). Six different concentrations of Percoll in phosphate-buffered saline (PBS) 10% fetal calf serum (FCS) were used (37.5%, 40%, 42.5%, 45%, 47.5%, and 60%). Fractions recovered at each interface from the top to the bottom of the gradients were numbered F1 to F5. The low buoyant-density F1 fraction, primarily constituted of dead cells, was discarded.

Flow cytometric analyses of $\Delta\Psi$m and of phosphatidylserine externalization

To evaluate changes in inner mitochondrial transmembrane potential $\Delta\Psi$m, cells were stained for 15 minutes at 37° with 40 nmol/L of the potential sensitive fluorescent dye DiOC$_6$ (3.3′-diethyloxacarbocyanine) from Molecular Probes. Phosphatidylserine externalization was detected by staining the cells with annexin V-FITC from Euromedex (Souffelweyersheim, France).

Hypodiploid cell assessment and microscopic detection of chromatin condensation

Cells (5×10^5) were washed in PBS with 5.5 mmol/L glucose and fixed overnight in ethanol (70% in water, at 4°C). Cells were then resuspended in 0.5 mL PBS containing 50 µg/mL propidium, 100 U/mL RNAse A (Sigma) and incubated for 1 hour at room temperature. The DNA content of 10^4 cells was monitored by cytofluorometry using a Coulter Epics profile II analyzer. To assess chromatin condensation, cells were fixed with 3% paraformaldehyde and incubated for 10 minutes at room temperature with 5 µmol/L 4′,6-diamino-2-phenylindole, dihydrochloride (DAPI, from Molecular Probes). Cells were rinsed, resuspended in Mowiol mounting medium, and analyzed by conventional (Leica Microsystèmes, Rueil-Malmaison, France) or confocal fluorescence microscopy.

Subcellular fractionation and immunoblotting

T cells ($5\text{-}10 \times 10^6$) were washed twice in PBS and resuspended in 500 µL of ice-cold extraction buffer[23] containing 220 mmol/L mannitol, 68 mmol/L sucrose, 50 mmol/L PIPES-KOH, pH 7.4, 50 mmol/L KCl, 5 mmol/L sodium EGTA, 2 mmol/L MgCl$_2$, 1 mmol/L dithiothreitol (DTT), and a cocktail of protease inhibitors (from Boehringer Mannheim, Meylan, France). After incubation on ice for 30 minutes, cells were homogenized with 60 pestle strokes of a glass homogenizer (Polylabo, Strasbourg, France). Unbroken cells and nuclei were pelleted by centrifugation at 760g for 10 minutes at 4°C. The resulting supernatants were centrifuged at 10 000g for 15 minutes to yield S10 supernatants and pellets enriched in mitochondria. The latter was resuspended in extraction buffer supplemented with 1% Triton X-100. The S10 supernatants were further centrifuged at 100 000g for 1 hour and the final S100 supernatants were either used as such or concentrated for 2 hours at 4°C on a 3 mw cut-off Centricon apparatus (Amicon Bioseparation, Millipore, ST Quentin en Yvelines, France). S100 and mitochondrial fractions were stored at −80°C.

Immunoblot analyses

Five to 20 µg of S100 cytosolic extracts and 5 µg of mitochondrial extracts were separated by sodium dodecyl sulfate-polyacrylamide gel electrophoresis (SDS-PAGE; 12% polyacrylamide) and transferred onto a polyvinylidene difluoride (PVDF) membrane (Immobilon-P, Millipore). After overnight incubation in PBS containing 3% bovine serum albumin (BSA) and 0.1% Tween 20, the membranes were incubated for 2 hours at room temperature with rabbit anti-AIF serum (1:2000 diluted), with anticytochrome c (1:2000) or with anticytochrome c oxidase (1:500). The blots were stripped by using a Western blot recycling kit (Euromedex) and reprobed with antiactin (1:500). The immunoreactive proteins were visualized by using horseradish peroxidase-coupled (HRP) goat antimouse IgG (Amersham, Les Ulis, France) or HRP-conjugated sheep antirabbit IgG (Biotest, BUC, France) and enhanced chemiluminescence detection system (ECL kit, Amersham). To evaluate PARP cleavage, 3×10^5 cells were

washed and solubilized in 10 μL Laemmli buffer. Cell lysates were then subjected to 8% SDS-PAGE and electroblotted onto a PVDF membrane. Blots were stained with anti-PARP (1:10 000) and revealed as above.

Confocal laser scanning microscopy analysis of cytochrome c and AIF localization

Cells were fixed with 3% paraformaldehyde in PBS for 30 minutes at 4°C, washed with PBS, and incubated with ClNH$_4$ (50 mmol/L) before being permeabilized with 0.05% Triton X-100 for 5 minutes at room temperature. After 3 washings, the cells were incubated for 1 hour at 4°C with rabbit anti-AIF and with mouse anticytochrome c, respectively, diluted at 1:200 and 1:100 in PBS supplemented with 0.5% BSA and 2% FCS. The cells were stained with fluorescein isothiocyanate (FITC)-conjugated AffiniPure goat antirabbit IgG and tetrarhodamine isothiocyanate (TRITC)-conjugated AffiniPure donkey antimouse IgG from Jackson Immunoresearch Laboratories (Immunotech, Luminy-Marseille, France). For localization of mitochondria, the cells were loaded with the mitotracker CMXRos red dye (Molecular Probes) before fixation, permeabilization, and labeling with the desired FITC-conjugated AffiniPure antibodies. Cells were examined using a CLSM confocal microscope (Leica).

Field inversed gel electrophoresis (FIGE)

One percent agarose plugs containing 1×10^6 cells were digested with proteinase K (0.5 mg/mL) at 37°C for 48 hours in the presence of 0.5 mol/L EDTA and 10 mg/mL lauroyl sarcosine. This step was followed by electrophoresis for 24 hours in 1% agarose gels using a FIGE mapper equipment from Bio-Rad Laboratories (Ivry Sur Seine). The gels were run for 24 hours in $0.5 \times$ TBE buffer (pH 8.3) at 170 V with a ramping rate changing from 5 to 15 seconds. Molecular weight standards (midrange PFG marker I) were purchased from Biolabs (Ozyme, Montigny le Bretonneux).

Results

Fractionation according to density of activated T-cell populations exposed to CD2 apoptotic signaling: definition of a commitment phase of apoptosis and comparison with anti-CD95-treated T cells

Within 2 hours following the receipt of CD2 apoptotic signal, in vitro activated T cells begin to shrink without losing membrane integrity and without exposing phosphatidylserine. Previous studies have determined that full-blown apoptosis occurs later, yielding after 4 hours approximately 30% to 40% apoptotic cells (with low $\Delta\Psi m$), which rapidly become permeable to trypan blue.[6] These observations led us to postulate that the first 2 hours of CD2 stimulation corresponded to a commitment phase and that initiation of cell shrinkage was one of the events characterizing commitment to apoptosis. A starting population of large activated T cells, homogeneous in terms of cell size, was isolated as F2-I cells in the low buoyant density fraction of a discontinuous density Percoll gradient. This F2-I cell population was then exposed for 2 hours to CD2 apoptotic signaling and, after extensive washing, fractionated on a second Percoll gradient into 5 fractions (F2-II to F5) displaying progressive increase in density and progressive decrease in cell volume (Figure 1A) and forward side scatter (Figure 1D). Control F2-I cells that had not been exposed to apoptotic insult remained at the low buoyant density level of the secondary gradients. Immediately after fractionation, most cells were viable as assessed by trypan blue exclusion and morphologic examination. When replaced for 16 hours in medium containing IL-2, large cells of the F2-II fraction remained viable, whereas in the subsequent fractions, increasing proportions of cells underwent apoptosis, yielding 35 ± 11% dead cells in F3, 58 ± 9% in F4, and 81 ± 7% in F5. The carry-over of residual anti-CD2 mAb did
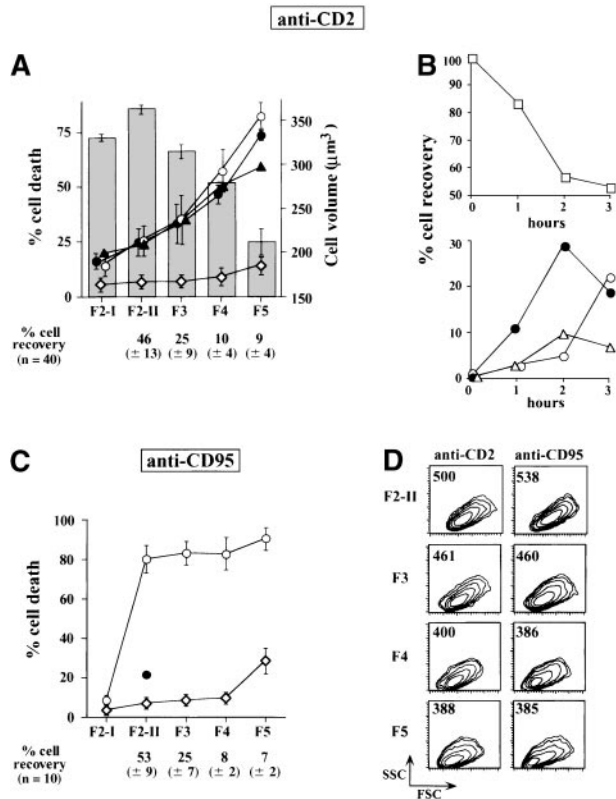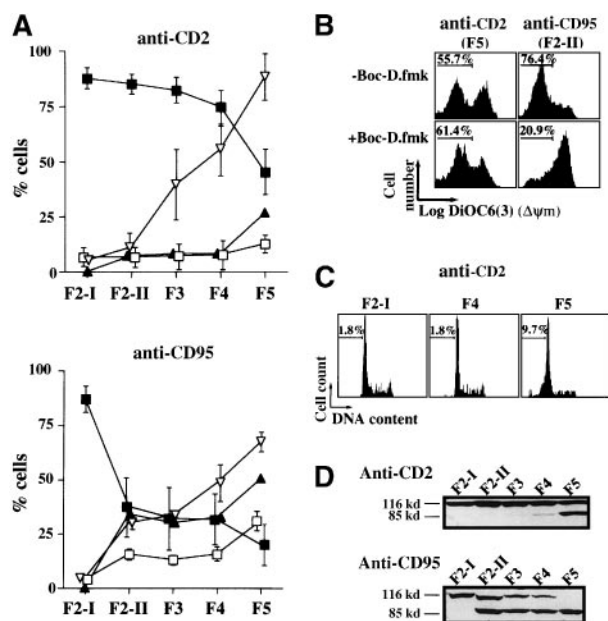

Figure 1. Fractionation of T cells after apoptotic induction. Activated T-cell populations exposed for 2 hours to CD2 or CD95 apoptotic induction and fractionated according to density on discontinuous Percoll gradients give rise to fractions progressively enriched in cells committed to apoptosis. (A) Homogeneous populations of large activated T cells (F2-I) obtained from the low buoyant density fractions of a first primary Percoll gradient were exposed for 2 hours to CD2 mAb (D66 +T11$_1$, 2 μg/mL) and were then fractionated again on secondary Percoll gradients to yield fractions F2-II, F3, F4, and F5 with decreasing cell volumes. Columns are mean cell volumes ± SD of determinations performed in 3 different experiments, as measured by using a Coulter counter and a channelyser. ◇---◇ indicates percent dead cells in the fractionated cell populations 2 hours after apoptotic induction, just after their recovery from the gradients, as assessed by trypan blue uptake and cell morphology (n = 40); ○---○, percent dead cells in fractionated cell populations replaced after washing in culture for 18 hours in IL-2 containing medium (n = 10); ●---●, percent dead cells in cells exposed to 50 μmol/L BOC-D.fmk during apoptotic induction and during subsequent culture in IL-2 containing medium (n = 3); ▲---▲, percent dead cells similarly exposed to 50 μmol/L Z-VAD.fmk. Values are means ± SD. (B) Activated (F2-I) T cells exposed for various periods of time to anti-CD2 mAb. At each time point, the percentages of cells recovered in the F2-II (□---□), F3 (●---●), F4 (△---△), and F5 (○---○) Percoll fractions were estimated. It is seen that the percentages of F2-II cells progressively decreased within 2 hours, whereas the percentages of F3, and to a lesser extent, those of F4 and F5 cells concomitantly increased. After 3 hours, the percentages of F2-II cells were stabilized, but a further rise in F5 cells occurred at the expense of F3 and F4 cells. (C) Fractionation of F2-I cells treated for 2 hours with an anti-CD95 at 250 ng/mL (n = 10). Symbols are the same as in panel A. Cells treated in parallel with 50 μmol/L BOC-D.fmk did not shrink and were therefore recovered in majority in the low buoyant fraction (F2-II) of the secondary Percoll gradients (●). (D) Forward scatter (FSC) analysis showing the reduction of cell size from F2-II to F5. Numbers refer to the mean forward scatter. SSC, side scatter.

not account for cell death because subjecting F2-I cells to a short acid pulse (pH 3, 1 minute on ice), at the end of the signalization period, removed all residual membrane-bound CD2 antibodies but did not modify the number of cells recovered in each fraction, nor the rate of cell death occurring thereafter (not shown). This indicated that the apoptotic process was launched despite interruption of the apoptotic insult. Kinetic experiments, carried out to examine the distribution of anti-CD2-treated cells in the gradient fractions over time (Figure 1B), strongly supported the notion that F3 and F4 cells were intermediary between F2 and F5 cells. The

presence of BOC-D.fmk or Z-VAD.fmk (50 μmol/L, to target most caspases) during the entire experimental procedure did not alter the distribution of condensed cells along the density gradients nor the percentages of cells committed to death in each fraction. Thus, the successive cell populations recovered from Percoll gradients after a short period of CD2 apoptosis induction were progressively enriched in cells committed to caspase-independent death. In the F2-I population subjected to CD95 ligation for 2 hours, the fractionation procedure gave rise to cells mostly committed to death, irrespective of their density. As expected, anti-CD95-induced cell death was strongly inhibited by the caspase inhibitor BOC-D.fmk (Figure 1C).

Partial chromatin condensation precedes ΔΨm collapse, PARP cleavage activity, and large scale DNA fragmentation in anti-CD2 treated cells

Using the lipophilic cationic fluorochrome $DiOC_6(3)$, which localizes to mitochondria as a consequence of $\Delta\Psi m$, we observed that the vast majority of cells in fractions F2-II to F4 exhibited, 2 hours after CD2 apoptotic induction, a high mitochondrial transmembrane potential, similar to that of the starting F2-I population. F5 was the sole fraction displaying $\Delta\Psi m$ collapse (with only about 45% $DiOC_6^{3high}$ cells versus about 88% in control F2-I, Figure 2A). As previously reported,[6] the loss of $\Delta\Psi m$ in this fraction was caspase-independent (not prevented by BOC-D.fmk, Figure 2B). From F2-II to F4, there was no significant generation of hypodiploid cells and in cells exposing phosphatidylserine on their surface. A small increase in the percentages of hypodiploid cells and annexin V^+ cells was, however, observed in F5 (Figure 2A,C).

Figure 2. Apoptotic alterations among the fractionated cell populations of activated T lymphocytes recovered 2 hours after their exposure to CD2 and CD95 apoptotic stimuli. (A) ■---■ indicates percent cells with high ΔΨm as measured in each fraction with $DiOC_6$ 3; ▽---▽, percent cells with condensed nuclei as visualized by DAPI staining; □---□, percent hypodiploid cells; ▲---▲, percent annexin-V-positive cells. Values are means ± SD of 20 determinations in the CD2 apoptotic system and of 10 determinations in the CD95 system. B) Effect of 50 μmol/L BOC-D.fmk on the occurrence of ΔΨm disruption in F5 cells of the CD2 system and in F2-II cells of the CD95 system. Data shown are representative of 3 different experiments. (C) Propidium iodide staining of DNA from ethanol-permeabilized cells. Values indicate the percentages of hypodiploid cells (linear scales are represented). (D) Total lysates of 5×10^5 cells were analyzed by Western blot using an anti-PARP mAb. Experiments are representative of 6 independent determinations.

Because no proteolytic cleavage of the nuclear PARP into its 85-kd signature fragment (mainly performed by caspase-3 and caspase-7)[24] was detected from F2-II to F4, whereas it was detected in F5 (Figure 2D), one can conclude that the caspase cascade was not activated until F5. By comparison, all fractionated cell populations recovered 2 hours after CD95 cross-linking displayed PARP cleavage and most of them had lost their mitochondrial transmembrane potential. In activated T lymphocytes, caspase-8 is, in fact, very rapidly recruited to the death-inducing signaling complex (DISC) on CD95 ligation.[22] This indirectly causes mitochondrial damage and cytochrome c release through the cleavage and activation of the death agonist BID.[25,26]

One striking nuclear change observed in the fractionated cell populations generated 2 hours after CD2 apoptotic signaling was progressive chromatin condensation, starting from F3. Thus, $36 \pm 15\%$ cells with condensed chromatin were scored in F3 by DAPI staining, $51 \pm 12\%$ in F4, and $95 \pm 9\%$ in F5 (versus about 5% in F2-I, n = 3). Ultrastructural examination of the fractionated cell populations (Figure 3) gave a more precise insight into nuclear morphology, indicating that 45% F3 cells and approximately 64% F4 cells had their heterochromatin condensed in discrete clumps abutting the nuclear membrane, whereas more condensed chromatin was seen in F5 cells. The presence of 50 μmol/L BOC-D.fmk during apoptosis signaling did not affect the partial chromatin condensation detected in F3 and F4 cells. This caspase inhibitor, however, prevented the advanced chromatin condensation detected in F5. Moreover, BOC-D.fmk inhibited all signs of nuclear apoptosis in anti-CD95-treated cells. We wondered whether large-scale chromatin fragmentation, which precedes internucleosomal fragmentation,[27] would coincide with the chromatin condensation seen in the CD2 system. However, no cleavage of DNA could be detected by FIGE from F2-II to F4 fractions of anti-CD2-treated cells, whereas cleavage to large kilobase pair sized fragments (50 kbp) was generated in F5 (Figure 4A). BOC-D.fmk inhibited the formation of these fragments (Figure 4B), corroborating the notion that large-scale DNA fragmentation may, in certain models, strictly depend on upstream caspase activity.[28,29]

On the whole, it appears that in the CD2 apoptotic system, the commitment phase to apoptosis, represented by F3 and F4 cells, is characterized by a reduction in cell size and by partial chromatin condensation, both being caspase independent. The subsequent execution phase of apoptosis is represented by frankly shrunken F5 cells, an important proportion of which displays caspase-independent $\Delta\Psi m$ loss and caspase-dependent nuclear events such as advanced chromatin condensation, large-scale DNA fragmentation, and PARP cleavage. In our experimental conditions, the execution phase was already at work in F2-II cells generated after CD95 signaling, as evidenced by the early $\Delta\Psi m$ loss affecting the majority of cells, and by PARP degradation. These events preceded cell shrinkage and advanced chromatin condensation, because only about 27% of F2-II cells displayed chromatin condensation, and this at a rather low extent (Figure 3).

Subcellular redistribution of AIF but not cytochrome c during the commitment phase of CD2-induced apoptosis

Subcellular fractionation of F3 to F4 cells (pooled to gain sufficient material), followed by immunoblot detection, did not allow detection of significant mitochondrial release of cytochrome c (Figure 5A), even when the S100 cytosolic extracts were concentrated up to 4-fold (data not shown), demonstrating the exclusive mitochondrial localization of cytochrome c in those cells. Adequacy of the subcellular fractionation procedure was assessed by using an

A

B
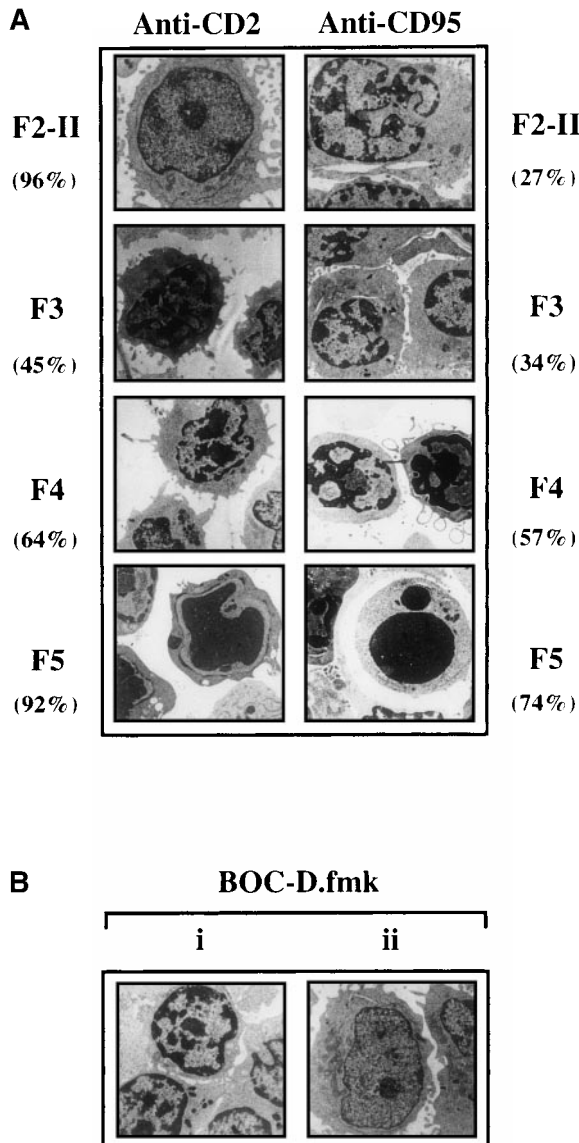
Figure 3. Ultrastructural changes occurring in the fractionated cell populations recovered 2 hours after apoptotic induction. (A) Sizeable proportions of activated T cells sedimenting in the F3 and F4 fractions of Percoll gradients after CD2 signaling display partial chromatin condensation. F2-I cells were exposed for 2 hours to anti-CD2, fractionated on density Percoll gradients, and examined by electron microscopy. Values inside the brackets are the percentages of cells displaying the same morphology as that represented in the pictures. (Bi) In the CD2 system, the presence of BOC-D.fmk (50 µmol/L) during apoptotic induction does not prevent the appearance of F5 cells with partial chromatin condensation, contrasting with the strong condensation seen in F5 cells generated in the absence of caspase inhibitor. (Bii) Cells treated with anti-CD95 in the presence of BOC-D.fmk retain a normal nuclear morphology and are still recovered in the low buoyant density fraction of Percoll gradients (at the level of F2-II).

anticytochrome oxidase mAb. In anti-CD95-treated cells, the release of cytochrome c into the cytosol already occurred in F2-II. We also examined by this technique whether mitochondrial AIF was released into the cytosol, using a rabbit antiserum to AIF. The specificity of anti-AIF detection was assessed in whole cell lysates by comparison with the preimmune serum obtained from the same rabbit (Figure 5B). Two forms of AIF were apparently recognized by the anti-AIF serum in SDS-PAGE analysis, one with an apparent 67-kd molecular mass, which corresponded to the migration of recombinant AIF (Figure 5C), and the other with an apparent 57-kd molecular mass. Detection of both forms was strongly attenuated

by preincubating the anti-AIF serum with a cocktail of AIF-derived peptides (Figure 5B). The molecular mass of recombinant AIF, deduced from the cDNA incoding AIF[14] and confirmed by mass spectrometry (not shown), is 57 kd. Its apparent higher molecular weight detected in SDS-PAGE may be due to ionic interaction with the gel matrix, as shown for another ferredoxin oxidoreductase.[30] Variations in the isoelectric points of AIF molecules might account for the differential migration patterns in SDS-PAGE. After CD2 apoptotic signaling, AIF was detected in the cytosol of pooled F3 to F4 cells but not in the cytosol of control F2-I cells or of F2-II cells. Data not shown indicated that the mitochondrial extracts from F3 to F4 cells still contained AIF. These data suggested that at least part of AIF was released from mitochondria during the commitment phase of apoptosis in anti-CD2-treated cells, whereas cytochrome c was retained in these organelles. In F2-II cells from anti-CD95-treated cells, which served as positive controls, both cytochrome c and AIF were released into the cytosol.

The respective cellular localizations of cytochrome c and AIF were further examined by laser scanner confocal microscopy in anti-CD2-treated cells that were simultaneously labeled with anti-cytochrome c and anti-AIF. The immunostaining of untreated F2-I cells demonstrated a punctate staining pattern for cytochrome c that matched the staining of AIF, consistent with the localization of these molecules in mitochondria (Figure 6A, B). This was confirmed by loading the cells with Mitotracker Red CMXRos, which localizes to mitochondria, and by staining cytochrome c or AIF in green. In this case, the punctate red staining pattern of CMXRos perfectly matched that of cytochrome c or AIF (not shown). After CD2 apoptotic signaling, cytochrome c remained in the mitochondria of all fractionated populations except F5 in which a diffuse distribution pattern throughout the cytosol was observed, even when apoptotic induction was performed in the presence of BOC-D.fmk or of Z-VAD.fmk (to ensure that most caspases would be inhibited; Figure 6C). In contrast, AIF was translocated earlier, as deduced from the diffuse anti-AIF staining already exhibited by the large majority ($\geq$ 95%) of F3 cells but not by F2-II cells, not committed to death. In some F3 cells, AIF was detected in the cytosol and to a lesser extent in the nucleus, whereas in F4 and F5 cells, it was detected equally well in the cytosol and the nucleus, consistent with the translocation of AIF through the cytosol toward

A   **B**
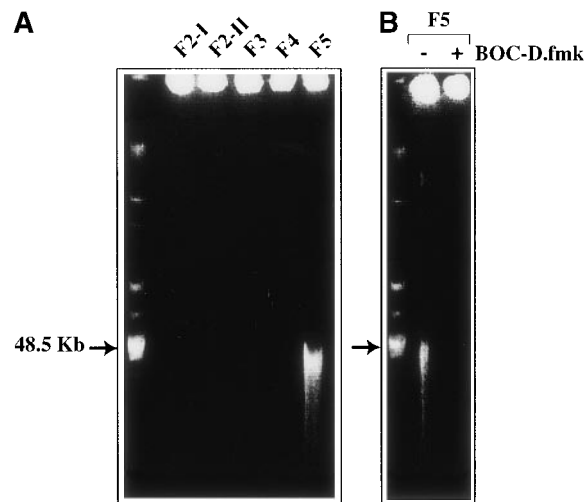
Figure 4. DNA cleavage. (A) Large-scale DNA fragmentation does not occur in F3 and F4 cells committed to apoptosis after CD2 apoptotic induction but does occur in a BOC-D.fmk inhibitable manner. (B) F5 cells entered the execution phase. Genomic DNA from 2×10^6 cells of each Percoll fraction was analyzed by pulse-field gel electrophoresis.

the nucleus.[14] The increased intensity of anti-AIF staining after release from mitochondria may reflect a better accessibility of the antigens recognized by the AIF antiserum because no increase in the total amount of AIF could be detected by Western blot analysis in any cell lysate, when compared to the lysates of control F2-I cells (not shown). As observed for cytochrome c, BOC-D.fmk and Z-VAD.fmk had no effect on AIF redistribution (Figure 6C), indicating that this was a caspase-independent phenomenon. On the whole, the release of AIF from mitochondria is an early and apparently selective event because it occurs before the release of cytochrome c.

Volume cell loss, partial chromatin condensation, and release of AIF may be reversible at an early stage of caspase-independent cell death commitment

When added to large F2-I cells, 250 nmol/L staurosporine provoked within 2 hours the shrinkage of 70% or more of the cells in a caspase-independent manner (not prevented by BOC-D.fmk, not shown). When recovered in the high buoyant density fraction of Percoll gradients, those cells were similar in many aspects to the F4
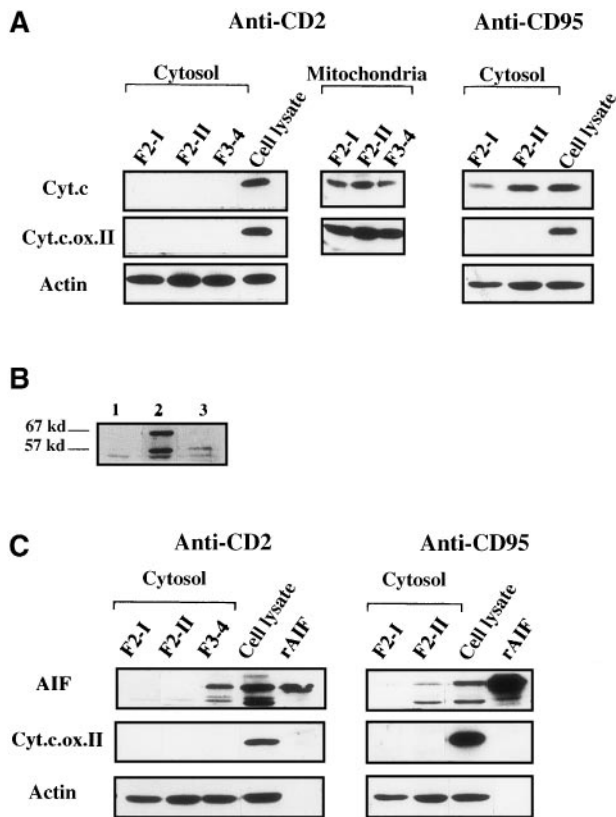

Figure 5. Mitochondrial AIF is released into the cytosol before cytochrome c in activated T cells subjected to CD2 apoptotic induction. (A) Cytosolic and mitochondrial extracts (5 μg) were prepared from cell populations that have been fractionated on Percoll density gradients after a 2-hour apoptotic induction with anti-CD2 or with anti-CD95. F3 and F4 cells were pooled to gain sufficient material. Total cell lysates were obtained from control activated F2-I cells. Immunoblots were probed with anticytochrome c (Cyt.c), with anticytochrome c oxidase subunit II (Cyt.c.ox.II) to detect the presence of mitochondrial material, or with antiactin to monitor protein loading in cytosolic extracts. (B) Specificity of AIF detection by immunoblot analysis. Total lysates of 5×10^5 activated T cells (F2-I) were probed with a preimmune rabbit serum (lane 1), or with a rabbit AIF antiserum (lane 2), or with the same AIF antiserum preincubated for 2 hours at 4°C under agitation with 1 mmol/L of a mixture of immunogenic AIF-derived peptides (amino acids 151-170, 166-185, 181-200). (C): Immunoblot analysis of cytosolic extracts from anti-CD2 and anti-CD95 treated cells by using AIF antiserum. Recombinant AIF (5 ng) and total cell lysates (5 μg) were used as positive controls. Data are representative of 5 experiments.
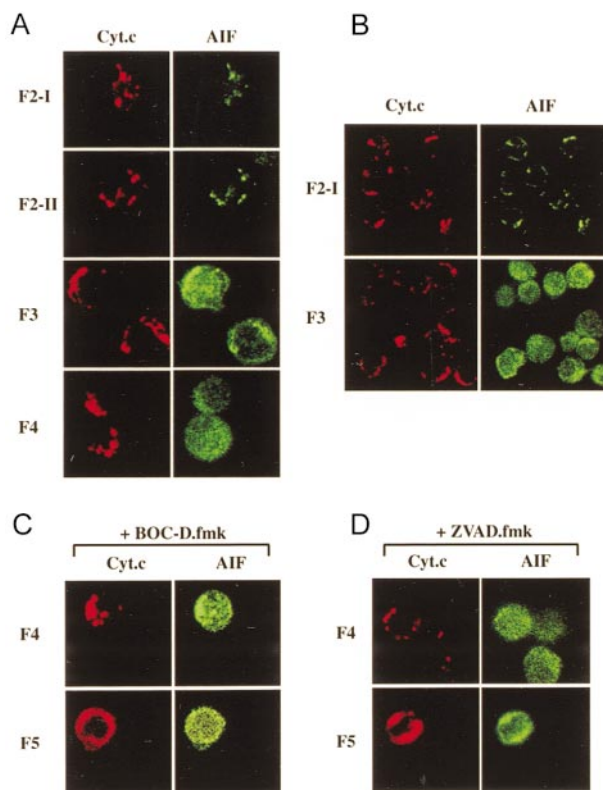
Figure 6. Differential subcellular localization of cytochrome c and AIF during the commitment phase of anti-CD2-induced apoptosis as visualized by confocal immunofluorescence microscopy. (A) In F3 and F4 cells, the punctate cytosolic distribution pattern of cytochrome c differs from the diffuse staining pattern of AIF throughout the cytosol and the nucleus. (B) A microscopic field displays several F3 cells to show that most of them exhibit a differential distribution pattern for AIF and for cytochrome. (C,D) The presence of BOC-D.fmk or Z-VAD.fmk (50 μmol/L) during apoptotic induction and Percoll fractionation does not prevent the mitochondrial release of cytochrome c and AIF in F5 cells.

cells generated after CD2 apoptotic insult: about half of them were committed to apoptotic death as determined by subsequent culture in IL-2-containing medium, but most displayed high $\Delta \Psi m$, moderate chromatin condensation, and diffuse immunostaining of AIF spread into the cytoplasm and the nucleus, contrasting with the punctate immunostaining of cytochrome c. Noteworthy, in both the CD2 and the staurosporine systems, the release of AIF from mitochondria was not necessarily correlated with cell death. For example, although at least 95% of F3 and F4 cells generated during CD2 apoptotic induction exhibited a diffuse immunostaining of AIF, only part of them (respectively, about 37% and about 50%) died in subsequent culture, suggesting that the apoptogenic factor AIF was degraded or held in check in the surviving cells. To study this aspect more in detail, we sought to obtain an homogenous population of cells just engaged in the commitment phase of apoptosis, assuming that a weak and brief apoptotic insult would induce AIF release, without causing cell death. This possibility was examined in staurosporine-treated cells, which allows control of the strength of the apoptotic stimulus. When activated T lymphocytes (F2-I cells) were exposed to only 100 nmol/L staurosporine for 2 hours, they shrunk and displayed partial condensation of their chromatin, events that were not inhibited by BOC-D.fmk (Figure 7A). The shrunken cells sedimented in the F4 and F5 fractions of Percoll density gradients, displayed a high mitochondrial transmembrane potential ($82 \pm 5\%$ $DiOC_6(3)^{high}$ cells for F4 and $70 \pm 5\%$ $DiOC_6(3)^{high}$ cells for F5, $n = 13$), had intact DNA as assessed by FIGE (Figure 7B), and lacked PARP cleaving activity (not shown).
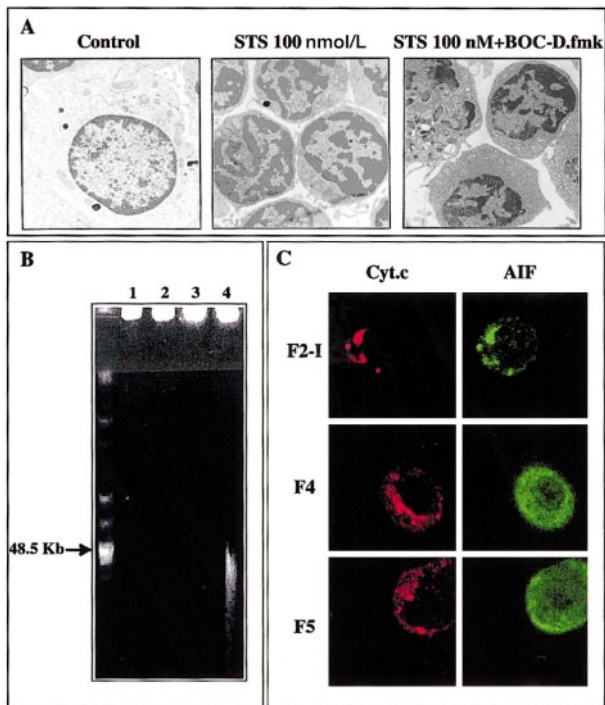
Figure 7. Characteristics of activated T cells subjected for 2 hours to 100 nmol/L staurosporine. (A) The ultrastructural changes seen in pooled F4 and F5 cells treated with staurosporine (STS), that is, cell shrinkage and partial chromatin condensation, persist in the presence of BOC-D.fmk. (B) Absence of large-scale DNA fragmentation in F4 and F5 cells contrasting with the approximate 50-kbp sized fragments seen in the F5 fraction of the CD2 system. 1, F2-I; 2, F4; 3, F5; 4, F5 generated after a 2-hour exposure to anti-CD2 (positive control). (C) Confocal immunofluorescence analysis of the localization of cytochrome c and AIF demonstrating that only mitochondrial AIF has been translocated to the cytosol and the nucleus.

Confocal laser scanning microscopy revealed that AIF had lost its punctate mitochondrial distribution and had been translocated to the cytosol and the nucleus, whereas cytochrome c was still retained in the mitochondria (Figure 7C). When washed and replaced in IL-2-containing medium, F4 and F5 cells did not undergo accelerated apoptosis as compared to control F2-I cells (a result of 6 different experiments). On the contrary, they dilated and recovered within 24 hours a normal size, and they continued to incorporate tritiated thymidine (70 800 ± 7308 cpm in F4 and 47 634 ± 7798 cpm in F5 versus 66 711 ± 10 726 in F2-I; mean ± SD of 3 experiments). The chromatin was no longer condensed (Figure 8A), and AIF immunostaining tended to regain a punctate distribution pattern, indicative of mitochondrial localization (Figure 8B). It therefore appears that the initial apoptogenic events triggered during the caspase-independent commitment phase to apoptosis in activated T lymphocytes may be reversible, provided the strength of the apoptotic stimulus is weak. Rescue mechanisms may be operative, in particular those that degrade AIF and repair the DNA alterations responsible for chromatin condensation.

Discussion

This study was aimed at deciphering the ordering of caspase-dependent and caspase-independent apoptogenic events that are triggered in activated T lymphocytes, using as apoptotic inducers anti-CD2 mAb and staurosporine. The latter stimulus was in particular suitable for analyzing the relationship between the strength of apoptotic induction and the ensuing events. We have set

up a system based on the isolation, according to density, of T cells progressively engaged in the apoptotic process. This allowed us to demonstrate that the commitment phase to apoptosis in the models investigated was caspase independent and that it was characterized by cell shrinkage, partial chromatin condensation, and translocation of AIF to the cytosol and the nucleus. The notion of commitment as such was deduced from the propensity of the cells to undergo accelerated cell death in culture, after removal of the apoptotic stimulus. Release of cytochrome c from mitochondria occurred at a more advanced stage of apoptosis, concurrently with $\Delta\Psi$m collapse and PARP cleavage activity, indicating that the cells had entered the execution phase of apoptosis. We have also demonstrated that the initial events of the commitment phase were reversible at low apoptotic insult.

Most T lymphocytes located in the commitment phase of apoptosis displayed a high mitochondrial inner membrane potential. Significant $\Delta\Psi$m loss was only detected after 1 to 2 hours of further culture (not shown). Yet a mitochondrial response was detected during commitment to apoptosis, which consisted in the caspase-independent translocation of AIF from the intermembrane space of mitochondria to the cytosol and the nucleus. This release was selective because cytochrome c was retained in the mitochondria of the very same cells as examined by laser scanning confocal
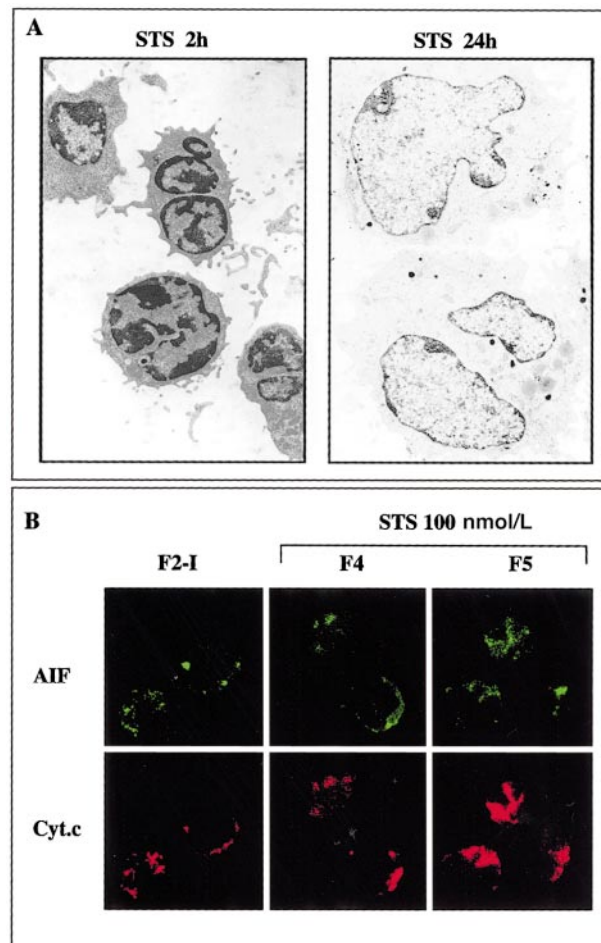
Figure 8. Reversibility of the morphologic alterations and of mitochondrial AIF release induced at low apoptotic insult. (A) F2-I cells that have been treated with 100 nmol/L staurosporine (STS) for 2 hours were washed and cultured for 24 hours in IL-2-containing medium. The electron micrographs show that the shrunken cells with partially condensed chromatin generated after 2 hours of apoptotic induction recover within 24 hours a normal aspect provided staurosporine is removed. (B) Confocal microscopy analysis showing that AIF tends to recover a punctated mitochondrial localization 24 hours after the removal of staurosporine (compare with Figure 7C).

microscopy and Western blot analysis. Therefore, the initial mitochondrial release of AIF appears not to be dependent on the overall release of intermembrane proteins, as is the case for apoptotic cells with swollen mitochondria, the outer membranes of which can be physically disrupted.[31] Instead, the lymphocytes that have entered the apoptotic pathway possessed mitochondria that were structurally intact as viewed by electron microscopy. That AIF was released without occurrence of the major mitochondrial perturbation represented by $\Delta\Psi$m collapse is at odds with previous studies.[14,32] However, mitochondrial dysfunction, due to subtle changes in $\Delta\Psi$m (not detectable by standard methods), may account for the mitochondrial release of AIF in T cells committed to apoptosis. Such subtle changes have been detected in isolated mitochondria incubated with Bax, a proapoptotic member of the Bcl-2 family.[33] Usually, insertion of Bax at μmol/L concentrations into isolated mitochondria results in $\Delta\Psi$m collapse and in cytochrome c release,[34,35] events that are associated with the interaction of Bax with components of the mitochondrial PT complex.[35-37] However, Pastorino and coworkers[33] have shown that at nmol/L concentrations, Bax does not induce detectable mitochondrial depolarization. Yet, several mitochondrial intermembrane space proteins are released (although not completely), including cytochrome c and adenylate kinase.[33] This release is due to transient and nonsynchronous opening and closing of the PT pores of a fraction of mitochondria, hardly detected by standard methods, but readily detected by using the cyclosporin A-sensitive release of preloaded calcein. Such a scenario may well occur in the mitochondria of intact cells because Bax moves from cytosol to mitochondria after a death signal.[38] Not only would this scenario help in reconciling the opposite points of view existing in the literature about the temporal relationship between cytochrome c release and $\Delta\Psi$m loss (see the review by Bernardi et al[39]), but it could also explain why AIF is released from mitochondria of cells with high $\Delta\Psi$m. However, if such were the case, the question remains of the reason why AIF and cytochrome c were not translocated simultaneously in the lymphocytes committed to apoptosis. This important question awaits elucidation.

The partial condensation of the chromatin observed in the nuclei of the lymphocytes committed to apoptosis was caspase independent, allowing us to discard the intervention of caspase-activated factors involved in chromatin condensation, namely caspase-activated DNAse (CAD),[40] caspase-6,[41] and the nuclear factor acinus.[42] Recombinant AIF directly causes chromatin condensation in isolated nuclei, and microinjected AIF antiserum prevents the nuclear effects (peripheral chromatin condensation and digestion of chromatin into 50-kbp fragments) induced by staurosporine in intact cells.[14] Released endogenous AIF might therefore account for chromatin condensation in the lymphocytes committed to death of our system. Note that cleavage of DNA into 50-kbp fragments was not detected in these lymphocytes, unless they had entered the execution phase of apoptosis cells. But in this case, caspase activity was clearly upstream of large scale DNA fragmentation, in line with other cell models.[28,29] It is possible that in situ the effects of released AIF might be subjected to cell type-specific regulation mechanisms with regard to chromatin condensation and DNA fragmentation, and that caspases may be differentially involved in these effector events. The causal relationship between the mitochondrial release of AIF and the early nuclear manifestations of apoptosis in activated T lymphocytes remains to be established. As to volume loss induced by apoptotic inducers, it is believed to be tightly linked to enhanced K^+ efflux.[43] Shrunken lymphocytes

display both decreased intracellular $[K^+]$ and caspase-dependent or independent $\Delta\Psi$m loss.[44,45] However, in the committed cells of our study, the overall mitochondrial transmembrane potential was normal. It would be interesting to measure $[K^+]$ in these populations and establish the temporal relationship between the expected K^+ efflux and the release of AIF, the sole indication thus far of mitochondrial perturbation in our determinations.

A most striking result observed in this study was the reversibility of cell shrinkage, of chromatin condensation, and of mitochondrial release of AIF, provided the strength of the stimulus was low and its application of short duration. After cessation of apoptotic insult, cells pretreated with 100 nmol/L staurosporine for 2 hours recovered a normal morphology within 18 hours in proliferated as well as control cells. AIF was no longer present in the cytosol and the nucleus, but instead was primarily localized in mitochondria, as visualized by confocal microscopy. When higher concentrations of staurosporine were used (250-500 nmol/L for 2 hours), the vast majority of shrunken cells displayed a diffuse distribution pattern of AIF throughout the cytosol and the nucleus, but only half of them were committed to death. Similarly, in most F3 and F4 cells of the CD2 system, AIF exhibited a uniform cellular distribution but important proportions of those cells survived after removal of anti-CD2 mAb. This suggests that rescue mechanisms were counteracting the death process and that at low apoptotic insult they were able to save a majority of cells, whereas at higher (or prolonged) apoptotic insult they became overwhelmed. The fact that released AIF had disappeared from the cytosol of saved cells also suggests that AIF was rapidly degraded. Some recent studies have demonstrated that the cytochrome c release[46,47] and the initial collapse of $\Delta\Psi$m occurring in certain cell death-inducing conditions[48,49] may be reversible. In our setting, the reversal of chromatin condensation and of cell shrinkage further emphasize the diversity of repair mechanisms (still to be investigated) within the different compartments of cells committed to apoptosis.

In the lymphocytes of our study, $\Delta\Psi$m loss and mitochondrial cytochrome c release were coincident with the entry in the execution phase of apoptosis as evidenced by PARP cleavage activity. Both apoptogenic events still occurred in the presence of BOC-D.fmk or Z-VAD.fmk. They could be followed, in these conditions, by an entirely caspase-independent cell death process.[6] It is now admitted that when caspase activity is not inhibited, multiple interconnected amplification loops, either caspase-dependent or caspase-independent, are involved in most apoptotic models, including CD95-induced apoptosis.[50,51] In our attempt to define the ordering of caspase-dependent and caspase-independents apoptogenic events that are triggered in T lymphocytes by signals that do not rely on the "death receptors" of the tumor necrosis factor-receptor family, we have characterized a caspase-independent commitment phase to apoptosis. These data might apply to the caspase-independent cell death triggered in $CD4^+$ T lymphocytes via the coreceptor of HIV-1, namely CXCR4,[10] and by HIV-1 infection.[52] In addition, the notion of reversible commitment to apoptosis might help developing strategies to prevent undesired cell death.

Acknowledgments

References

1. Wyllie AH, Kerr JFR, Currie AR. Cell death: the significance of apoptosis. Int Rev Cytol. 1980;68: 251-306.

2. Cryns V, Yuan J. Proteases to die for. Genes Dev. 1998;12:1551-1570.

3. Xiang J, Chao DT, Korsmeyer SJ. BAX-induced cell death may not require interleukin 1 beta-converting enzyme-like proteases. Proc Nat Acad Sci U S A. 1996;93:14559-14563.

4. Sarin A, Williams MS, Alexander-Miller MA, Berzofsky JA, Zacharchuk CM, Henckart PA. Target cell lysis by CTL granule exocytosis is independent of ICE/CED-3 family protease. Immunity. 1997;6:209-215.

5. McCarthy NJ, Whyte MKB, Gilbert CS, Evan GI. Inhibition of Ced-3-related proteases does not prevent cell death induced by oncogenes, DNA damage, or the Bcl-2 homolog Bak. J Cell Biol. 1997;136:215-227.

6. Déas O, Dumont C, MacFarlane M, et al. Caspase-independent cell death induced by anti-CD2 and staurosporine in activated human peripheral T lymphocytes. J Immunol. 1998;161: 3375-3383.

7. Lavoie JN, Nguyen M, Marcellus RC, Branton PE, Shore GC. E4orf4, a novel adenovirus death factor that induces p53-independent apoptosis by a pathway that is not inhibited by zVAD-fmk. J Cell Biol. 1998;140:637-645.

8. Monney L, Otter I, Olivier R, et al. Defects in the ubiquitin pathway induce caspase-independent apoptosis blocked by Bcl-2. J Biol Chem. 1998; 11:6121-6131.

9. Borner C, Monney L. Apoptosis without caspases: an inefficient molecular guillotine? Cell Death and Differentiation. 1999;6:497-507.

10. Berndt C, Möpps B, Angermüller S, Gierschik P, Krammer PH. CXCR4 and CD4 mediate a rapid CD95-independent cell death in CD4+ T cells. Proc Natl Acad Sci U S A. 1998;95:12556-12561.

11. Weil M, Jacobson MD, Raff MC. Are caspases involved in the death of cells with a transcriptionally inactive nucleus? Sperm and chicken erythrocytes. J Cell Sci. 1998;111:2707-2715.

12. Bernardi P. Mitochondrial transport of cations: channels, exchangers and permeability transition. Physiol Rev. 1999;79:1127-1155.

13. Zamzami N, Marchetti P, Castedo M, et al. Reduction in mitochondrial potential constitutes an early irreversible step of programmed lymphocyte death in vivo. J Exp Med. 1995;181:1661-1672.

14. Susin SA, Lorenzo HK, Zamzami N, et al. Molecular characterization of mitochondrial apoptosis-inducing factor. Nature. 1999;397:441-446.

15. Wolf BB, Green DR. Suicidal tendencies: apoptotic cell death by caspase family proteinases. J Biol Chem.1999;274:20049-20052.

16. Susin SA, Lorenzo HK, Zamzami N, et al. Mitochondrial release of caspase-2 and -9 during the apoptosic process. J Exp Med. 1999;189:381-394.

17. Mancini M, Nicholson DW, Roy S, et al. The caspase-3 precursor has a cytosolic and mitochondrial distribution: implications for apoptotic signaling. J Cell Biol. 1998;140:1485-1495.

18. Samali A, Cai J, Zhivotovski B, Jones DP, Orrenius S. Presence of a preapoptotic complex of pro-caspase-3, Hsp60 and Hsp10 in the mitochondrial fraction of Jurkat cells. EMBO J. 1999; 18:2040-2048.

19. Xanthoudakis S, Roy S, Rasper D, et al. Hsp60 accelerates the maturation of procaspase-3 by upstream activator proteases during apoptosis. EMBO J. 1999;18:2049-2056.

20. Wyllie AH, Kerr JFR, Currie AR: Cell death: the significance of apoptosis. Int Rev Cytol. 1980;68: 251-306.

21. Cohen GM, Sun XM, Fearnhead H, et al. Formation of large molecular weight fragments of DNA is a key committed step of apoptosis in thymocytes. J Immunol. 1994;153:507-516.

22. Scaffidi C, Kirchhoff S, Krammer PH, Peter ME. Apoptosis signaling in lymphocytes. Curr Opin Immunol. 1999;11:277-285.

23. Bossy-Wetzel E, Newmeyer DD, Green DR. Mitochondrial cytochrome c release in apoptosis occurs upstream of DEVD-specific caspase activation and independently of mitochondrial transmembrane depolarization. EMBO J. 1998;17:37-49.

24. Tewari M, Quan LT, O'Rourke K, et al. Yama/CPP32β, a mammalian homolog of CED-3, is a crmA-inhibitable protease that cleaves the death substrate poly (ADP-ribose) polymerase. Cell. 1995;81:801-809.

25. Li H, Zhu H, Xu CJ, Yuan J. Cleavage of BID by caspase 8 mediates the mitochondrial damage in the Fas death pathway of apoptosis. Cell. 1998; 94:491-501.

26. Luo X, Budiharjo I, Zou H, Slaughter C, Wang X. Bid, a Bcl2 interacting protein, mediates cytochrome c release from mitochondria in response to activation of surface death receptors. Cell. 1998;94:481-490.

27. Oberhammer FA, Wilson JW, Dive C, Morris ID, Hickman JA. Apoptotic death in epithelial cells: cleavage of DNA to 300 and /or 50 kb fragments prior to or in the absence of internucleosomal fragmentation. EMBO J. 1993;12:3679-3684.

28. Samejima K, Toné S, Kottke TJ, et al. Transition from caspase-dependent to caspase-independent mechanisms at the onset of apoptosis execution. J Cell Biol. 1998;143:225-239.

29. Sakahira H, Enari M, Ohsawa Y, Uchiyama Y, Nagata S. Apoptotic nuclear morphological change without DNA fragmentation. Curr Biol. 1999;9: 543-546.

30. Böhme H, Schrautemeier B. Comparative characterization of ferredoxins from heterocysts and vegetative cells of Anabaena variabilis. BBA. 1987;891:1-7.

31. Vander Heiden MG, Chandel NS, Williamson EK, Schumacker PT, Thompson CB. Bcl-XL regulates the membrane potential and volume homeostasis of mitochondria. Cell. 1997;91:627-637.

32. Susin SA, Zamzani N, Castedo M, et al. Bcl-2 inhibits the mitochondrial release of an apoptogenic protease. J Exp Med. 1996;184:1331-1342.

33. Pastorino JG, Tafani M, Rothman RJ, Marcineviciute A, Hoek JB, Farber JL. Functional consequences of the sustained or transient activation of Bax on the mitochondrial permeability transition pore. J Biol Chem. 1999;274:31734-31739.

34. Jürgensmeier JM, Xie Z, Devereaux Q, Ellerby L, Bredesen D, Reed JC. Bax directly induces release of cytochrome c from isolated mitochondria. Proc Natl Acad Sci U S A. 1998;95:4997-5002.

35. Narita M, Shimizu S, Ito T, et al. Bax interact with the permeability transition pore to induce permeability transition and cytochrome c release in isolated mitochondria. Proc Natl Acad Sci U S A. 1998;95:14681-14686.

36. Marzo I, Brenner C, Zamzami N, et al. Bax and adenine nucleotide translocator cooperate in the mitochondrial control of apoptosis. Science. 1998;281:2027-2031.

37. Shimizu S, Narita M, Tsujimoto Y. Bcl-2 family proteins regulate the release of apoptogenic cytochrome c by the mitochondrial channel VDAC. Nature. 1999;399:483-487.

38. Wolter KG, Hsu YT, Smith CL, Nechustan A, Xi XG, Youle RJ. Movement of Bax from the cytosol to mitochondria during apoptosis. J Cell Biol. 1997;139:1281-1292.

39. Bernardi P, Scorrano L, Colonna R, Petronilli V, Di Lisa F. Mitochondria and cell death: mechanistic aspects and methodological issues. Eur J Biochem. 1999;264:687-701.

40. Liu X, Pi P, Widlak P, et al. The 40-kDa subunit of DNA fragmentation factor induces DNA fragmentation and chromatin condensation during apoptosis. Proc Natl Acad Sci U S A. 1998;95:8461-8466.

41. Takahashi A, Alnemri ES, Lazebnik YA, et al. Cleavage of lamin A by Mch2α but not CPP32: multiple interleukin 1β-converting enzyme-related proteases with distinct substrate recognition properties are active in apoptosis. Proc Natl Acad Sci U S A. 1996;93:8395-8400.

42. Sahara S, Aoto M, Eguchi Y, Imamoto N, Yoneda Y, Tsujimoto Y. Acinus is a caspase-3 activated protein required for apoptotic chromatin condensation. Nature. 1999;401:168-172.

43. Yu SP, Yeh CH, Sensi SL, et al. Mediation of neuronal apoptosis by enhancement of outward potassium current. Science. 1997;278:114-117.

44. Dallaporta B, Hirsch T, Susin SA, et al. Potassium leakage during the apoptotic degradation phase. J Immunol. 1998;160:5605-5615.

45. Bortner CD, Cidlowski JA. Caspase independent/dependent regulation of K+, cell shrinkage, and mitochondrial membrane potential during lymphocyte apoptosis. J Biol Chem. 1999;274:21953-21962.

46. Chen Q, Takeyama N, Brady G, Watson AJM, Vive C. Blood cells with reduced mitochondrial membrane potential and cytosolic cytochrome c can survive and maintain clonogenicity given appropriate signals to suppress apoptosis. Blood. 1998;92:4545-4553.

47. Martinou I, Desagher S, Eskes R, et al. The release of cytochrome c from mitochondria during apoptosis of NGF-deprived sympathetic neurons is a reversible event. J Cell Biol.1999;144:883-889.

48. Kerr KM, Suleiman MS, Halestrap AP. Reversal of permeability transition during recovery of hearts from ischemia and its enhancement by pyruvate. Am J Physiol. 1999;276:496-502.

49. Minamikawa T, Williams DA, Bowser DN, Nagley P. Mitochondrial permeability transition and swelling can occur reversibly without inducing cell death in intact human cells. Exp Cell Res. 1999; 246:26-37.

50. De Maria R, Lenti L, Malisan F, et al. Requirement for GD3 ganglioside in CD95- and ceramide-induced apoptosis. Science. 1997;277:1652-1655.

51. Kawahara A, Ohsawa Y, Matsumura H, Uchiyama Y, Nagata S. Caspase-independent cell killing by Fas-associated protein with death domain. J Cell Biol. 1998;143:1353-1360.

52. Gandhi RT, Chen BK, Straus SE, Dale JK, Lenardo MJ, Baltimore D. HIV-1 directly kills by a Fas-independent mechanism. J Exp Med.1998;187: 1113-1122.